STRUCTURAL BIOLOGY

Volume 72 (2016)

Supporting information for article:

Structure of TSA2 reveals novel features of the active-site loop of peroxiredoxins

Maja Holch Nielsen, Rune Thomas Kidmose and Lasse Bohl Jenner

S1. Supporting results

S1.1. Changes in pH do not seem to affect the conformation the C-terminus of TSA2

Our structure shows that the C-terminus of TSA2 can exist in both an α-helical form and in an unfolded form in the reduced state, as also reported for other peroxiredoxins (Wang *et al.*, 2012; Perkins *et al.*, 2013), and in the disulphide form the C-terminal α-helix must be unfolded (Hall *et al.*, 2009). Furthermore our structure and a previous study by Perkins et al. indicate that the conformation of the C-terminus affects the flexibility of the C_p loop, and therefore the reactivity of the peroxidatic cysteine (Perkins *et al.*, 2013). The ease of unfolding of the C-terminus has also been implicated in the sensitivity towards hyperoxidation of the peroxidatic cysteine (Wood, Poole, *et al.*, 2003), which in turn has been linked to the switch to the high molecular weight chaperone form (Jang *et al.*, 2004; Chuang *et al.*, 2006). For several peroxiredoxins, changes in pH have been reported to affect the dimer/decamer equilibrium (Morais *et al.*, 2015; Bernier-Villamor *et al.*, 2004; Kristensen *et al.*, 1999), and for some peroxiredoxins low pH can induce the formation of the high molecular weight complexes (Saccoccia *et al.*, 2012; Radjainia *et al.*, 2015). We therefore found it interesting to investigate how changes in pH affect the C-terminal α-helix of TSA2.

TSA2 contains three tryptophan residues, Trp83, Trp161, and Trp173. Trp83 is buried and not expected to experience a change of environment upon oxidation or changes in the C-terminus. Trp161 and Trp173 are both located near the C-terminus, and could be expected to experience a change in environment with changes in the C-terminus. These tryptophans are therefore expected to be good probes for conformational changes in the C-terminus in a tryptophan fluorescence experiment. This was confirmed by measuring the fluorescence of dithiothreitol (DTT) and H_2O_2 treated wild type TSA2, which showed a shift in peak emission wavelength from 342 nm to 335 nm upon oxidation (Figure S4a), indicating that the tryptophans experiences a less polar environment upon oxidation. A similar shift was not observed for the C48S mutant, showing that the measured shift was most likely due to conformational changes associated with disulphide formation. The shift in fluorescence upon oxidation could be due to changes in oligomeric state or changes in the conformation of the C-terminus. We expect that changes in the C-terminal conformation is the most likely cause for the change in fluorescence, as the crystal structure of oxidized TSA2 reveals a decamer similar to the reduced state. The results therefore indicate that tryptophans 161 and 173 can be used as probes for conformational changes of the C-terminus. When pH was changed from 5.8 to 9.0 no fluorescence shift was observed for either H_2O_2 or DTT treated wild type or the C48S mutant (Figure S4a and Figure S5a.), indicating that pH does not affect the conformation of the C-terminus.

Circular Dichroism (CD) spectroscopy confirmed this, as changing the pH resulted in no significant changes of the CD spectra of either wild type or C48S mutant TSA2 (Figure S4b and Figure S5b)

whereas H_2O_2 treatment of wild type TSA2 did result in a change (Figure S4b). Again this change must primarily be due to conformational changes associated with disulphide formation, as only a very small change was observed for the C48S mutant (Figure S4b).

S2. Supporting methods

S2.1. Purification and oxidation of wild type TSA2

Wild type TSA2 was purified as described for the C48S mutant, but after size exclusion the protein was treated with 50 mM H_2O_2 at room temperature for 30 minutes to induce disulphide bond formation. The H_2O_2 was removed again using a PD-10 desalting column (GE healthcare), and the protein stored at -80^{o}C until use.

S2.2. Crystallization, data collection and data processing for oxidized wild type TSA2

Crystals of TSA2 wild type in the disulphide state were grown by sitting drop vapour diffusion by mixing 2 µL H_2O_2 treated protein (3.8 mg/mL) with 2 µL reservoir containing 6% (w/v) PEG20K, 0.2 M $MgCl_2$, and 0.1 M NaCitrate pH 5.
As for the C48S mutant, wild type crystals were cryo-protected by gradual soaking into 20% (v/v) glycerol in reservoir buffer and flash frozen in the cryo-stream.

The data was collected at the ID23 beam line at the ESRF, and the data was processed and merged with XDS and XSCALE respectively.

Contrary to the TSA2_C48S crystals, the TSA2 wild type crystals belong to the space group $P2_12_12_1$, and diffracted very anisotropically with resolution limits of approximately 6.3 Å, 5.2 Å, and 4.0 Å along the a, b, and c axes respectively. To correct for anisotropy, the UCLA MBI -Diffraction Anisotropy Server was used to perform Ellipsoidal Truncation and Anisotropic Scaling of the data (Strong *et al.*, 2006).

S2.3. Model-building and refinement of the oxidized wild type TSA2 structure

Molecular replacement and model refinement was done using the Phenix package.

For the wild type crystals, molecular replacement was performed using the anisotropy corrected data to 5 Å and the decamer of TSA2_C48S as search model, followed by a rigid body refinement with individual monomers as rigid bodies to ensure correct placement. The structure was then refined to 5 Å using non-crystallographic, secondary structure and ramachandran restraints. The density clearly show that the C-termini of several monomers have been displaced to allow the formation of a disulphide bond between cysteine 48 and cysteine 171 compared to the structure of the C48S mutant. The final model was refined to R_{work}/R_{free} values of 0.273/0.369, with most of the disulphides modelled (Cys48/A-Cys171/B, Cys48/B-Cys171/A, Cys48/F-Cys171/E, Cys48/G-Cys171/H,

Cys48/H-Cys171/G, Cys48/I-Cys171/J, and Cys48/J-Cys171/G). The model has been deposited with the PDB with PDB ID: 5EPT.

S2.4. CD spectroscopy and tryptophan fluorescence

CD spectroscopy was performed using a JASCO J-810 spectropolarimeter (Jasco Spectroscopic Co. Ltd., Japan) equipped with a Jasco PTC-423S temperature control unit set to 20^{o}C and a 1mm quartz cuvette. CD scans covering wavelengths from 190 to 250 nm were made with a scanning speed of 100nm/min, a band width of 2nm, and a response of 4 seconds. Oxidized samples were produced by treating purified protein with 50 mM H_2O_2 at room temperature for 30 minutes to induce disulphide bond formation, and reduced samples were left untreated in a buffer containing 2 mM DTT. Oxidized and reduced protein samples were diluted to a final concentration of 0.19 mg/mL in 0.1 M potassium phosphate buffer with pH values ranging from 5.8 to 8.0, or in 20mM Tris-HCl buffer with 100mM KCl and pH values ranging from 8.0-9.0. For reduced samples, 2mM DTT was also included in the buffer. To ensure a good signal to noise ratio, only data points with a High Tension value below 600 V were used in the analysis. The High Tension value is the voltage applied to the photomultiplier to obtain a constant current throughout the measurement of the spectrum.

The samples for tryptophan fluorescence were prepared as described for CD spectroscopy, but diluted to 0.04 mg/mL, and measured on a Cary Eclipse (Varian) fluorescence spectrophotometer. An excitation wavelength of 280 nm was used and emission measured from 300-450 nm.

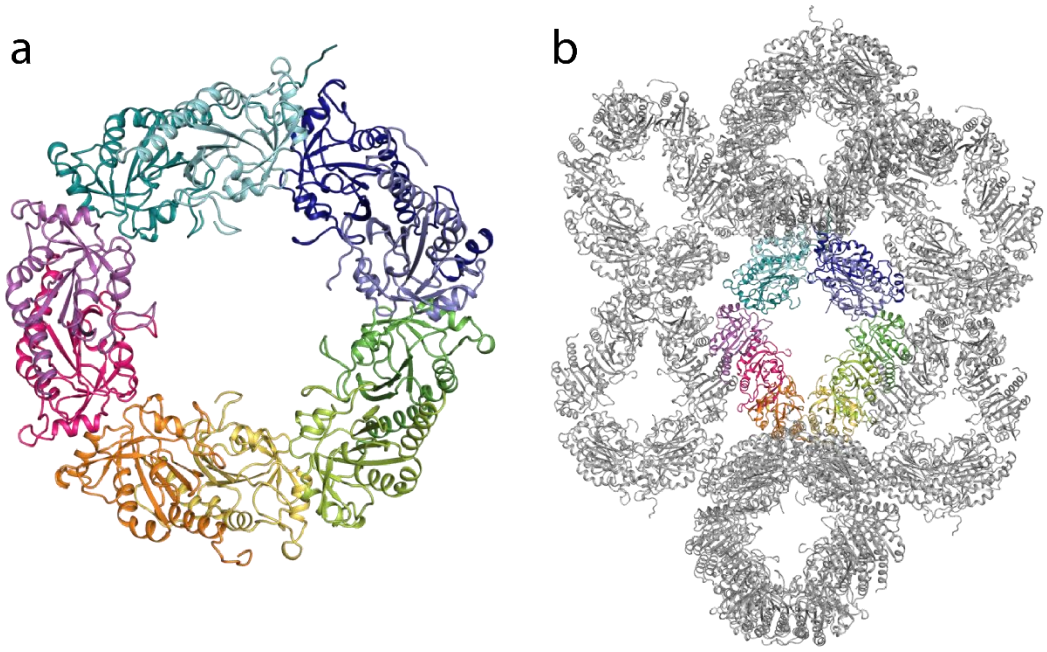

Figure S1 The TSA2_C48S decamer and it's crystallographic packing. a: The TSA2_C48S decamer with individual monomers coloured differently. Monomer A (dark blue), monomer B (light blue), monomer C (forest green), monomer D (lime green), monomer E (yellow), monomer F (orange), monomer G (hot pink), monomer H (magenta), monomer I (dark cyan), monomer J (light cyan). b: The nearest symmetry related molecules are shown in grey. The colour coding of the central decamer is as in a. The effects that the different C-terminal conformations and packing interactions have on the conformations of the C_p loops of the different monomers are shown in figure S2.

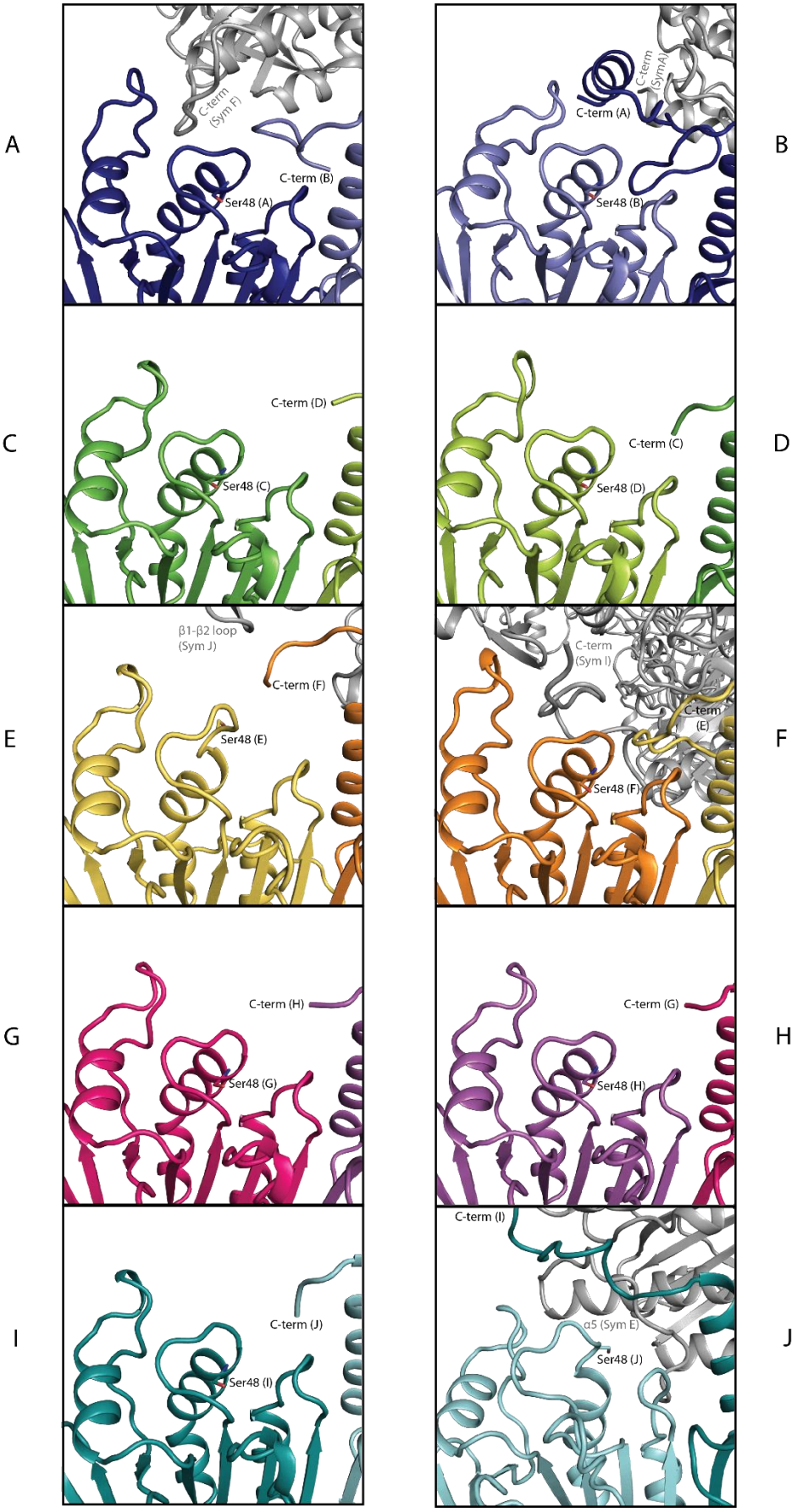
A
C-term (Sym F)
C-term (B)
Ser48 (A)
B
C-term (Sym A)
C-term (A)
Ser48 (B)
C
C-term (D)
Ser48 (C)
D
C-term (C)
Ser48 (D)
E
β1-β2 loop (Sym J)
C-term (F)
Ser48 (E)
F
C-term (Sym I)
C-term (E)
Ser48 (F)
G
C-term (H)
Ser48 (G)
H
C-term (G)
Ser48 (H)
I
C-term (J)
Ser48 (I)
J
C-term (I)
α5 (Sym E)
Ser48 (J)

Figure S2 Different C-terminal conformations and packing interactions allow different conformations of the C_p-loop to be stabilized in different monomers of the TSA2_C48S structure. The C_p-loops of the 10 monomers are shown along with the C-terminal part of the neighbouring monomer and any nearby symmetry related molecule (grey). Ser48 is shown as sticks to indicate the location of the C_p loop. The letters on the sides indicate which monomer the depicted C_p-loop belongs to. The colours of each monomer are as in figure S1. The C-terminus of monomer A is in the α-helical conformation. C_p-loops of Monomers E and J are in locally unfolded conformations. The different C-terminal conformations and their interactions with the C_p loop of the dimeric partner and with symmetry related molecules are summarized in table S1.

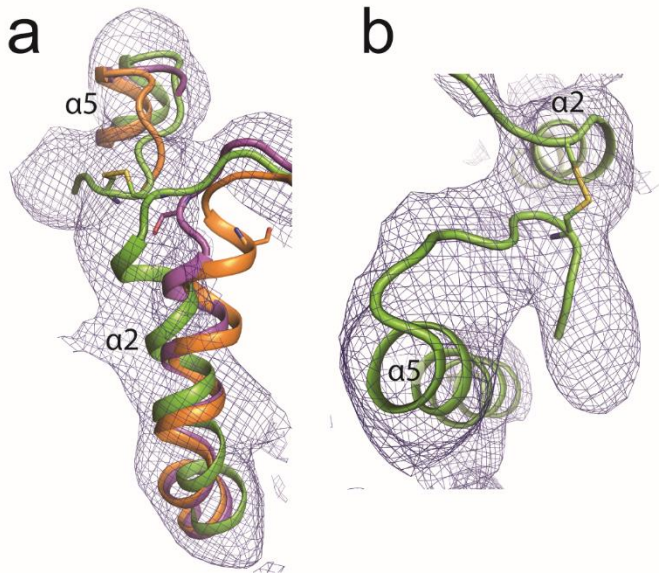

Figure S3 The disulphide state of wild type TSA2. a: Comparison the fully folded C_p loop (orange) and the locally unfolded C_p loop (magenta) of the TSA2_C48S mutant structure with the wild type TSA2 structure (light green). Cα –atoms of residues -1-149 from monomers B and J from TSA2_C48S and monomer J from the TSA2 structure were used for the superposition. The 2Fo-Fc electron density map calculated for wild type TSA2 has been contoured at 1.2 rmsd. It is clear that α2 is partly unwound and tilted in the disulphide state, unlike what has been seen for other 2-cys peroxiredoxins. b: Top view of the disulphide between C_p (Cys48) and C_r (Cys171) of wild type TSA2. C_p is found in α2 of monomer J and C_r in the C-terminus of monomer I, where I and J together form the functional dimer. The 2Fo-Fc map is contoured at 1.2 rmsd and clearly demonstrates the presence of the disulphide bond.

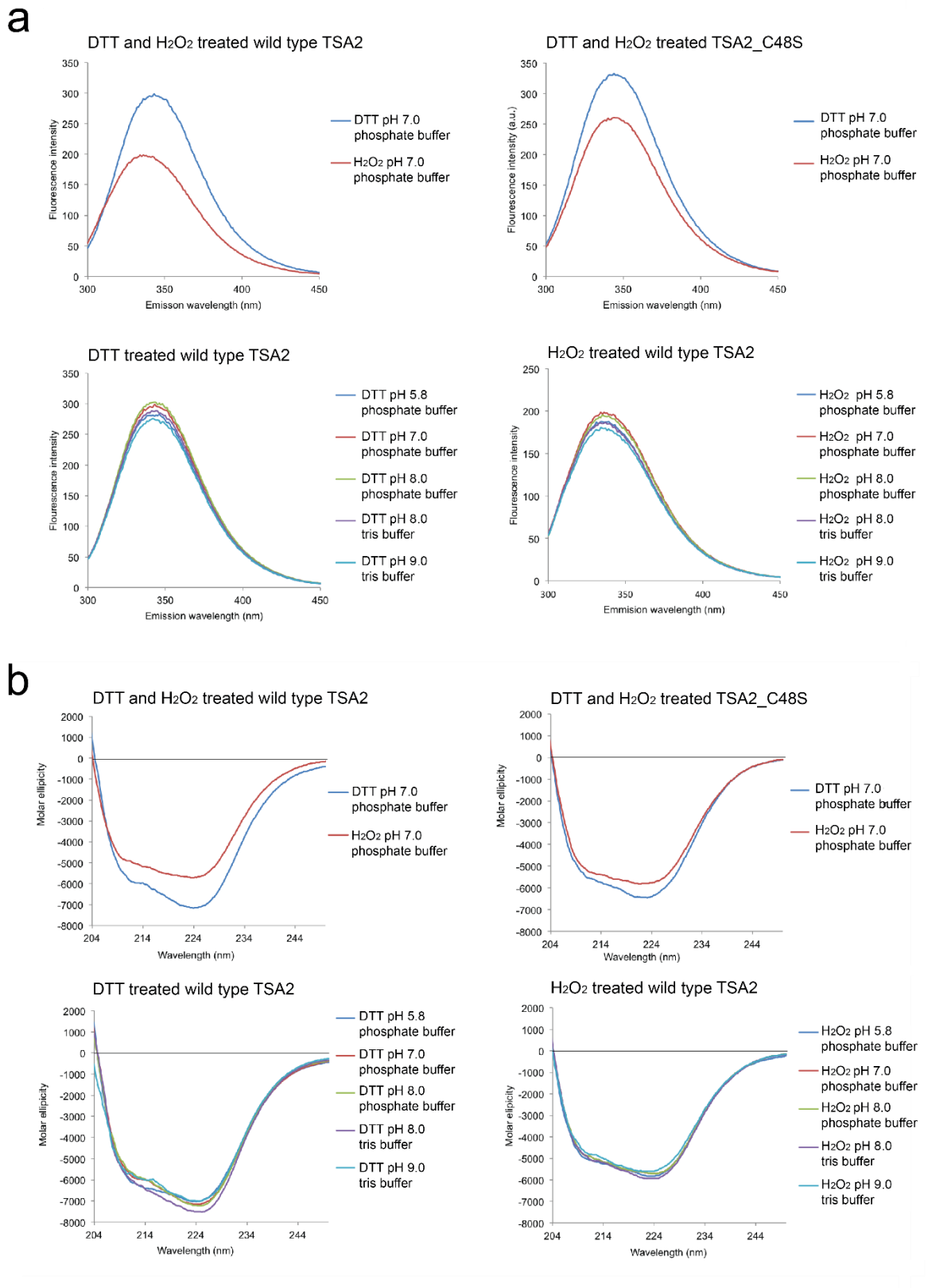

Figure S4 a: Tryptophan fluorescence was measured for DTT (blue) and H_2O_2 treated (red) wild type TSA2 (top left) and TSA2_C48S mutant (top right). For wild type TSA2 there is a shift in peak emission wavelength from 342 nm to 335 nm upon oxidation. As expected, a similar shift is not

observed for the TSA2_C48S mutant upon treatment with H_2O_2. The effect of pH changes was assessed by measuring tryptophan fluorescence for DTT treated wild type TSA2 (bottom left) and H_2O_2 treated wild type TSA2 (bottom right) at pH values ranging from 5.8 to 9.0. The buffers used (0.1 M potassium phosphate or 20 mM Tris with 100 mM KCl) are indicated in the figure. Changing pH from 5.8 to 9.0 did not cause a shift of emission wavelength for either reduced or oxidized wild type TSA2. b: CD spectrums of DTT (blue) or H_2O_2 (red) treated wild type TSA2 (top left) and TSA2_C48S mutant (top right) were measured as described in supporting methods in 0.1M potassium phosphate buffer, pH 7.0 with 2 mM DTT included for the reduced sample. For wild type TSA2 a change in the CD spectrum is observed upon oxidation indicating a change in secondary structure upon disulphide formation. For the C48S mutant only a minor change is observed upon H_2O_2 treatment. The effect of pH changes was assessed by measuring CD-spectra for DTT treated wild type TSA2 (bottom left) and H_2O_2 treated wild type TSA2 (bottom right) at pH values ranging from 5.8 to 9.0. The buffers used are indicated on the figure as for the tryptophan fluorescence experiments. pH changes in this interval do not appear to affect the secondary structure.

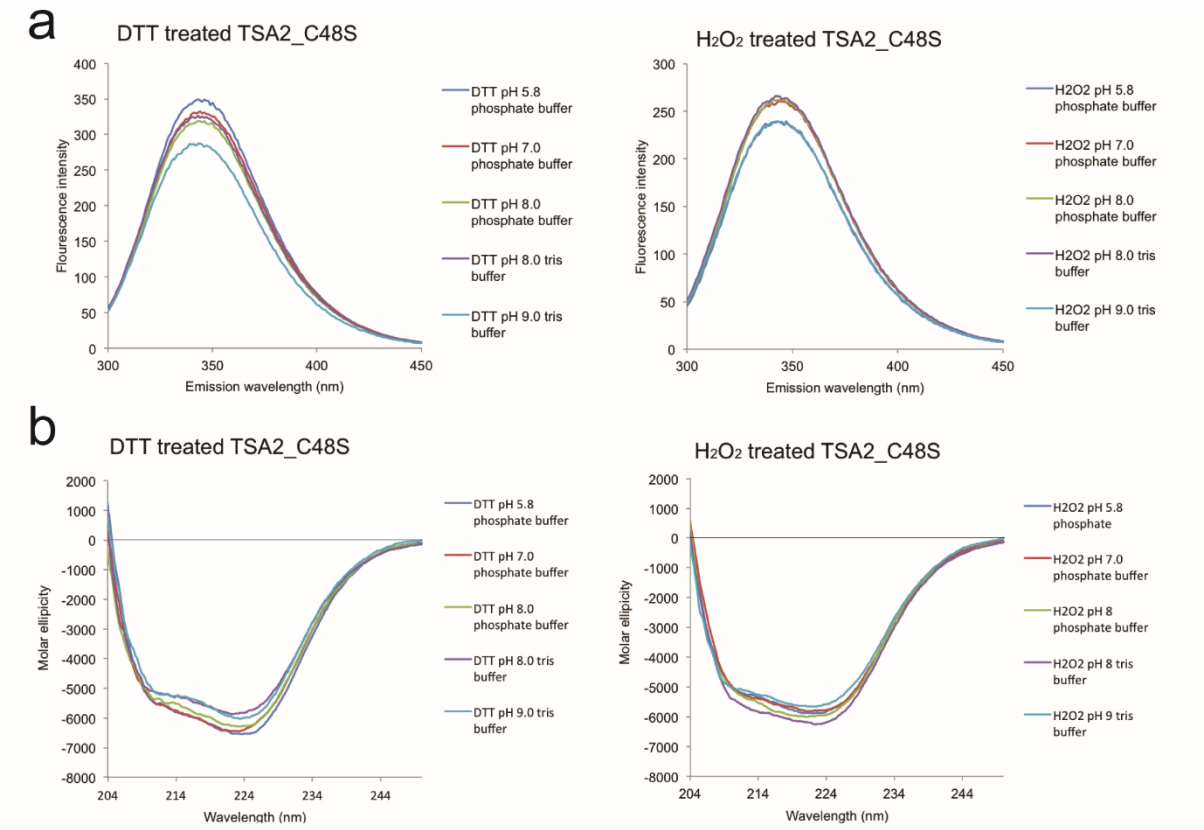

Figure S5 a: Tryptophan fluorescence of DTT treated (left) or H_2O_2 treated (right) TSA2_C48S was measured at different pH values ranging from 5.8-9.0 in phosphate or tris buffer as indicated. The DTT and H_2O_2 treated samples were prepared as described in supporting methods. b: CD Spectra of DTT treated (left) or H_2O_2 treated (right) TSA2_C48S measured in phosphate or tris buffer at different pH values ranging from 5.8 to 9.0.

Both CD spectroscopy and tryptophan fluorescence shows no significant change for TSA2_C48S with changing pH.

Table S1 Summary of C-terminal conformations and packing interactions.

Monomer	*Residues included in the model*	*C-terminal conformation*	*C-terminus packing against C_p-loop of dimeric partner*	*Interactions of C-terminus with symmetry related molecules*
A	-3 - 195	α-helix	C- terminus packs nicely and buries the C_p loop (46-50) of B.	Packs against C-terminus of A (176-179 interacts with 179-176 of A in symmetry related molecule)
B	0 - 175	Extended	Limited interactions with C_p loop of A. (168 of B can interact with 47 of A)	Packing interactions with C-terminal part of α2 (66-64) of F.
C	-3 - 168	Only few residues included	Limited interactions with C_p loop of D. (168 of C can interact with 47 of D)	Packing interactions with residues 154 of G and with 148 of H.
D	-3 - 166	Not included	No interactions with C_p loop of C	No packing interactions with symmetry related molecules.
E	-3 - 179	Extended	Some interactions with C_p loop of F. (168 and 170 of E can interact with 47 of F)	Packing interactions with C-terminal end of α5 and the following loop (154-168) of I on one side and the N-terminal end of α5 and the preceding loop (144-150) of J on the other side. As well as interactions with C_p- loop (48) of J.
F	-3 - 172	Extended	No interaction with C_p loop of E.	Packing interactions with the loop between β1 and β2 (21-22) and with α3 (78) of J. Also packing interactions with C_p loop (45) of A.
G	-3 - 167	Only few residues included	No interaction with C_p loop of H.	No packing interactions with symmetry related molecules.
H	-3 - 167	Only few residues included	No interaction with C_p loop of G.	No packing interactions with symmetry related molecules.
I	-3 - 182	Extended	Limited interactions with C_p loop of J. (169 and 175 of I can interact with 46 of J)	The C-terminus inserts itself between the C_p loop (44-46) and the loop following α3 (90-92) of F. Furthermore, residue 182 interacts with the loop between β1 and β2 (residues 21-22) of G.
J	-3 - 168	Only few residues included	Very weak/limited interactions with C_p loop of I. (168 of J can interact weakly with 47 of I)	No packing interactions with symmetry related molecules.

Table S2 Data collection, processing, structure solution, and refinement of oxidized TSA2, PDB ID: 5EPT

Values for the outer shell are given in parentheses.

*Data collection**	
Wavelength (Å)	0.8726
Resolution range	46.4-5.0 (5.2-5.0)
Space group	$P2_12_12_1$
Unit cell	
a, *b*, *c* (Å)	83.46, 167.21, 221.81
α, β, γ (°)	90, 90, 90
Total reflections	280358
Unique reflections	14005(1381)
Multiplicity	20
Completeness (%)	99.8(99.9)
Mean I/sigma(I)	13.98(2.78)
R_{meas}[a]	0.132 (1.250)
$CC_{1/2}$ [b]	0.999(0.982)
Refinement statistics	
R_{work}[c]	0.278 (0.338)
R_{free}[d]	0.367 (0.431)
Number of non-hydrogen atoms	13616
RMS (bonds)	0.007
RMS (angles)	1.13
Ramachandran favored (%)	93
Ramachandran allowed (%)	6.1
Ramachandran outliers (%)[e]	0.75

*) Data collection statistics is before Ellipsoidal Truncation and Anisotropic Scaling of the data.

a) $R_{meas} = \frac{\Sigma_{hkl}\sqrt{\frac{1}{n-1}}\Sigma_{j=1}^{n}|I_{hkl,j}-\langle I_{hkl}\rangle|}{\Sigma_{hkl}\Sigma_j I_{hkl,j}}$, where $I_{hkl,j}$ is the scaled intensity of the j[th] measurement, and I_{hkl} is the mean intensity for that reflection.

b) $CC_{1/2}$ is half dataset correlation coefficient (Karplus & Diederichs, 2012)

c) <sgmlfi>{R_{work}} = {{\mathop \sum \nolimits_{hkl} \left| {F_{hkl}^{obs} - F_{hkl}^{calc}} \right|} \over {\mathop \sum \nolimits_{hkl} F_{hkl}^{obs}}}</sgmlfi>

d) R_{free} is calculated as R_{work}, but with a test set of reflections comprising 5% of the data, not included in the refinement.

e) The 0.75% Ramachandran outliers correspond to 13 ramachandran outliers.

Table S3 The average B-factor of main chain atoms of the whole structure or residues 45-49 of chains A-J.

	Average main chain B-factor (Å^2)
Whole structure	60.0
Residues 45-49 of chain A	68.4
Residues 45-49 of chain B	57.2
Residues 45-49 of chain C	90.6
Residues 45-49 of chain D	79.3
Residues 45-49 of chain E	106.7
Residues 45-49 of chain F	71.0
Residues 45-49 of chain G	82.1
Residues 45-49 of chain H	79.1
Residues 45-49 of chain I	64.4
Residues 45-49 of chain J	73.1